

Sea ice, as the glacial cycles' climate switch, and interhemispheric thermohaline teleconnections

HEZI GILDOR, ELI TZIPERMAN

Environmental Sciences, Weizmann Institute of Science, Rehovot 76100, Israel

ABSTRACT. A box model combining the different physical components of the coupled ocean, atmosphere, sea-ice and land-ice climate system is used to study the possible role of sea ice in the glacial–interglacial oscillations. In this paper we investigate the teleconnection between the two hemispheres, and suggest a mechanism which can explain the observed Southern Ocean sea-ice variability during glacial–interglacial cycles. The teleconnection mechanism involves changes in the temperature of the water transported from the Northern to the Southern Hemisphere by the thermohaline circulation (THC), rather than the amplitude of the THC as has often been suggested. The sequence of events proposed by this model indicates that it would be especially interesting to obtain accurate information on the relative timing of sea-ice and land-ice variations. Fuller general circulation models and new sea-ice proxy data are needed to quantify the relative role of the proposed teleconnection mechanism.

1. INTRODUCTION

The glacial–interglacial cycles during the past million years were characterized by a pronounced time-scale of 100 kyr, with additional weaker spectral peaks at 41 and 23 kyr. Atmospheric CO₂ also underwent changes on the same time-scale, with lower concentration during glacial conditions (Petit and others, 1999). The existence of a dominant 100 kyr cycle in spite of the weak Milankovitch forcing at this frequency (Imbrie and others, 1993) prompted alternative theories such as jumps between stable modes of the ocean–atmosphere system (Paillard, 1998) and in particular of the thermohaline circulation (THC) (Broecker and Denton, 1989), non-linear transfer of power from higher-frequency Milankovitch forcing (Le Treut and Ghil, 1983) and more (Stokes, 1955; Saltzman, 1990; Muller and MacDonald, 1997). The asymmetric saw-tooth structure of the 100 kyr glacial cycles, with slow ice build-up and rapid terminations, was attributed to phase locking to Milankovitch solar variations (Saltzman, 1990), rapid transitions between unspecified multiple steady states of the climate system (Paillard, 1998), dust-loading albedo feedbacks (Peltier and Marshall, 1995) or ice-sheet instability (Pollard, 1983). The nearly synchronous climate variations in the Southern and Northern Hemispheres on the 100 kyr time-scale despite the asynchronous insolation forcing calls for some mechanism other than insolation.

Full general circulation models (GCMs) (Manabe and Broccoli, 1985) and intermediate models (Peltier and Marshall, 1995; Weaver and others, 1998) have been used to calculate quasi-steady-state snapshots of the climate for fixed glacial-like forcing and orbital parameters. Yet, due to the computational cost of GCMs, highly idealized models seem to have provided us with much of our present understanding of glacial cycle dynamics (Weertman, 1976; Le Treut and Ghil, 1983; Saltzman, 1990; Saltzman and Verbitsky, 1993; Ghil, 1994; Paillard, 1998; Loutre and Berger, 2000). Previously used simple models were able to obtain an impressive fit to

the observed proxy records (Saltzman and Verbitsky, 1993; Paillard, 1998). However, the somewhat vague and non-explicit representation of climate processes in these models does not enable them to propose specific detailed physical mechanisms responsible for the glacial cycle dynamics.

A physical model and mechanism for the 100 kyr glacial oscillations was presented in Gildor and Tziperman (2000, 2001), including simplified yet explicit model components for the oceanic meridional circulation, sea ice, land glaciers and atmosphere. For this study we improve the representation of the Southern Ocean dynamics. For simplicity, we force the model with seasonal varying insolation but without orbital varying parameters. The result is a plausible scenario for glacial oscillations, including the physical mechanisms involved in both the glacial and interglacial stages and the transitions between the states.

The main novel finding of the present study is a physical mechanism explaining the near synchrony in climate variation of the two hemispheres, despite the asynchronous radiation forcing (Clark and others, 1999). During interglacial periods, the stratification in the Southern Ocean is composed of cold fresh upper water above salty and warmer North Atlantic Deep Water (NADW) arriving to the Southern Ocean from the north. Note that this water mass is relatively warm also due to mixing with surface mid-latitude water on its way from the North Atlantic. We propose that during the build-up stage of Northern Hemisphere ice sheets the deep water formed in the North Atlantic becomes gradually colder, as suggested by proxy records (Schrag and others, 1996). Similarly, the mixing with cooler glacial-period surface water in mid-latitudes results in the subsurface deeper water arriving at the Southern Ocean colder and denser. The temperature and the amount of the upwelling water then play a key role in controlling the Southern Ocean sea-ice extent (Gordon, 1981; Martinson, 1990): the lower deep-water temperature results in a larger sea-ice extension during cold periods. The sea-ice albedo then induces strong cooling

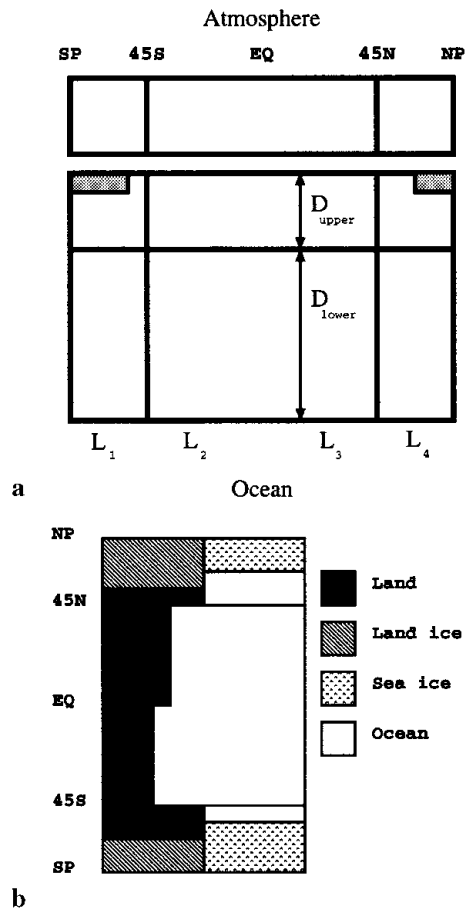


Fig. 1. The box model: (a) meridional cross-section of the box model. Shaded regions represent sea ice; (b) top view of the box model.

of the atmosphere above the Southern Ocean. Thus the teleconnection between the two hemispheres in this model is not a result of the THC intensity (Broecker and Denton, 1989), but mostly of the temperature of the water transported by the THC to the Southern Ocean.

2. THE MODEL

Our coupled meridional box model, schematically shown in Figure 1, is composed of ocean, atmosphere, sea-ice and land-ice models and is very similar to the one used and described in detail by Gildor and Tziperman (2000, 2001). We therefore describe the model briefly, emphasizing the changes made for the present study. The ocean is represented in our model by three surface boxes and three deep boxes, and represents both hemispheres. The polar boxes represent the regions between 45° and the poles, while the mid-latitude box includes the regions between 45° S and 45° N. The meridional circulation through the northern box is governed by a commonly used balance between the horizontal friction and the meridional pressure gradient (Stommel, 1961). The dynamics in the Southern Ocean, however, is different from that in the Northern Hemisphere. The upwelling of water in the south is the result of the westerly winds there, driving northward Ekman transport and thus upwelling in the Southern Ocean (Toggweiler and Samuels, 1993; Gnanadesikan, 1999). Because the exact dependency of the upwelling on factors such as the intensity of the wind and on sea-ice cover is still unclear, we have chosen to fix the intensity of the THC through the southern polar box to a specified value (of

14 Sv). The ocean temperature and salinity are driven by air–sea fluxes of heat and fresh water, as well as by fresh-water fluxes from land-ice ablation and runoff.

Sea ice forms when the ocean water temperature decreases below a critical freezing temperature, and melts above that temperature. Following the observed characteristic of sea ice in both hemispheres, the sea-ice cover is assumed to grow within the northern and southern polar ocean boxes with an initial thickness of 3 and 1.5 m, respectively, and then to become thicker if the entire polar box is sea-ice covered (the sea ice never fills the entire polar boxes in the simulations presented below). Sea-ice presence and evolution affect the surface albedo and the salinity budget in the ocean, and also affect the air–sea fluxes (heat flux and evaporation) by partially insulating the ocean from the atmosphere. The equation of state is the full non-linear equation recommended by Unesco (1981).

The atmospheric model is also similar to that used by Gildor and Tziperman (2000, 2001). The lower surface of each atmospheric box is a combination of ocean, land, land ice and sea ice, each with its specified albedo. The averaged potential temperature of each atmospheric box is calculated based on the energy balance of the box, taking into account: (1) incoming solar radiation using a box albedo calculated according to the relative fraction of each lower surface type in the box; (2) outgoing longwave radiation at the top of the atmosphere; (3) heat flux into the ocean; (4) meridional atmospheric heat transport.

The meridional atmospheric moisture transport plays an important role in the temperature–precipitation feedback which, in turn, is responsible for the glacial–interglacial oscillations in our model. The precipitation–temperature feedback suggests that the increase in accumulation rate of snow over land glaciers due to a temperature increase outweighs the corresponding increase in ablation and melting. Indeed, many proxy records (Lorius and others, 1985; Alley and others, 1993; Cuffey and Clow, 1997) and GCMs (Charles and others, 1994) clearly show that snow accumulation over high-latitude glaciers has increased during warm periods, sometimes by a factor of 4 and up to an order of magnitude. This is probably the result of both temperature changes and changes in the atmospheric circulation (such as movements of the storm track). We use a simple parameterization which accounts for these observations (Gildor and Tziperman, 2000, 2001) and results in an increased meridional transport of humidity during warmer periods, contributing to the temperature–precipitation feedback also used by Källén and others (1979), Ghil and others (1987) and Ghil (1994). Results of GCM experiments (Charles and others, 1994) and some proxy records (Hebbeln and others, 1994) indicate that a significant amount of the precipitation feeding the glaciers comes from high latitudes (e.g. the Norwegian and Greenland seas). Therefore another source of precipitation over the land-ice sheets in the polar boxes is local evaporation from the part of the polar box ocean not covered by sea ice. Sea-ice cover during cold periods reduces this source of moisture (Stokes, 1955; Donn and Ewing, 1966; Ruddiman and McIntyre, 1981), thus complementing the temperature–precipitation feedback.

The outgoing longwave radiation in the *i*th box is $H_{\text{out}} = P_{\text{lw}}^i \sigma \theta^4$, where σ is the Stefan–Boltzmann constant and P_{lw}^i is an emissivity coefficient which in principle depends on cloud cover, aerosol, CO₂ concentration, etc., and is therefore allowed here to vary from box to box.

We have introduced a few improvements to the model for the purpose of the present study. First, the sea-ice cover in the Southern Ocean in our previous applications of this model was nearly full, with very little glacial–interglacial or seasonal sea-ice cover variability there. In order to study the teleconnection between the hemispheres, this aspect of the simulation must be improved. Another change has been to incorporate the latent heat in the Haney-type air–sea heat flux parameterization (Haney, 1971), instead of the more explicit latent-heat flux representation used previously. Finally, we have changed the model to incorporate the important contribution of shortwave radiation to sea-ice thermodynamics, and the model now uses 15% of the incoming shortwave radiation, H_{in} , for melting of sea ice if and where it exists. The amount of shortwave radiation which reaches the sea-ice surface, namely, $(1 - \alpha_c)(1 - \alpha)H_{in}$, where α is the sea-ice albedo and α_c is the cloud albedo, is divided between a part which goes back to the atmosphere as longwave radiation and turbulent heat flux, a part which is transmitted to the ocean through the ice and a part which directly causes sea-ice melting. Note that if the sea ice is not very thin and if brine pockets are neglected, the fraction of shortwave radiation transmitted to the ocean through the sea ice is quite small. This transmission of shortwave radiation to the ocean, which is also further reduced by the insulating effect of snow over the sea ice, is therefore neglected in our model and is added instead to the heating of the atmosphere. This heating does eventually contribute to the heating of the ocean by the atmosphere via the Haney-type air–sea heat flux we use. The shortwave radiation term which influences the energy balance of the sea ice can be written as (Maykut and Perovich, 1987)

$$(1 - \alpha_c)(1 - \alpha)(1 - i_0)H_{in},$$

where i_0 is the fraction of the net shortwave radiation that does not contribute directly to surface melting. Although α_c , α and i_0 in reality depend on variables such as the type of the ice, its age, etc., we took them to be constants with values of 0.30, 0.65 and 0.39, respectively, giving together $(1 - \alpha_c)(1 - \alpha)(1 - i_0) = 0.15$, i.e. 15% of the incoming shortwave radiation.

The model for the northern land-ice sheets, whose slow evolution provides the 100 kyr time-scale in our model, is zonally symmetric and assumes perfect plasticity so that its height is parabolic in latitude (Weertman, 1976; Ghil, 1994). The relatively rapid bedrock deflection (Weertman, 1976; Källén and others, 1979; Peltier, 1994; Peltier and Marshall, 1995) as well as the elevation desert effect and dust-loading feedback (Peltier and Marshall, 1995) are neglected. The ice sheet grows due to precipitation in the polar boxes, assumed to be evenly distributed in the box. Ice sheets can decrease as a result of ablation, ice-runoff and calving processes. In order for the ice sheet to grow, there should be excess of accumulation over ablation whether the ablation is constant or variable. We choose the simplest assumption (of constant ablation) that allows us to investigate the sea-ice switch mechanism. More complex models of the ice-sheet mass balance (Huybrechts and Oerlemans, 1990; Huybrechts and others, 1991) also indicate that the assumption of constant ablation is fairly reasonable as a first approximation during the glacial–interglacial cycles. In addition, while investigating the role of orbital forcing in Gildor and Tziperman (2000) we have allowed the ablation to be a function of the summer insolation, and the oscillation mechanism has not been affected much (although the shape of the land-ice oscillation has become more realistic).

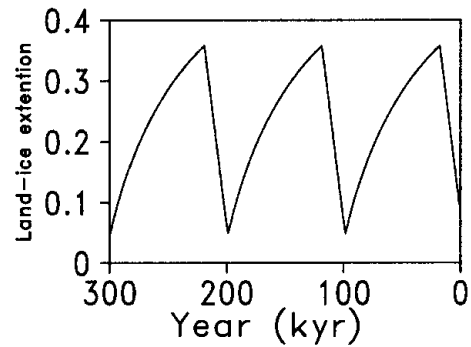


Fig. 2. Time series of model land-ice extent in the northern polar box as a fraction of land area.

Temperature-dependent ablation may be important in human-induced greenhouse scenarios (Huybrechts and Oerlemans, 1990) but is likely to be weaker than the temperature–precipitation feedback for colder climates during the past 900 kyr (Källén and others, 1979; Huybrechts and others, 1991).

As observed changes in land ice-sheet cover between glacial and interglacial occurred mostly in the Northern Hemisphere (Crowley and North, 1991), land ice in the south-

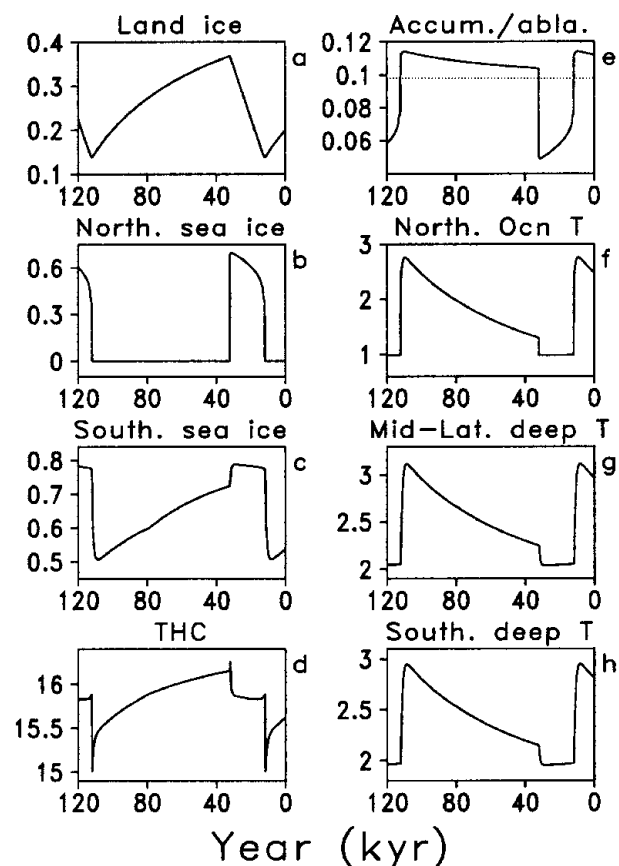


Fig. 3. Time series of model result during one complete glacial–interglacial cycle. (a) Northern land-ice extent as a fraction of the polar land box area; (b) northern sea-ice extent as a fraction of polar ocean box area; (c) southern sea-ice extent as a fraction of polar ocean box area; (d) THC through the northern polar boxes ($10^6 \text{ m}^3 \text{ s}^{-1}$); (e) source term (solid line) and sink term (dashed line), for northern land glacier ($10^6 \text{ m}^3 \text{ s}^{-1}$); (f) temperature in the northern upper polar oceanic box ($^{\circ}\text{C}$); (g) temperature in the mid-latitude deep oceanic box ($^{\circ}\text{C}$); (h) temperature in the southern deeper polar oceanic box ($^{\circ}\text{C}$).

ern box is constrained in the model to cover an area equal to Antarctica, and not to change during the model integration.

3. RESULTS

The model simulation of land-ice extent (Fig. 2) has roughly the general characteristics of the observed proxy records of land-ice volume, in terms of the 100 kyr cycles with their sawtooth structure. Let us briefly describe the mechanism of a complete glacial–interglacial cycle as analyzed in detail in Gildor and Tziperman (2000, 2001): as the land ice begins to grow from its minimum point (Fig. 3a; 110 kyr) the ocean in the northern polar box is ice-free (Fig. 3b) and sea-ice extent in the Southern Ocean is minimal (Fig. 3c). The atmospheric (not shown) and ocean temperatures (Fig. 3f) in the northern box are rather mild. Snow accumulation over glaciers exceeds the ablation, melting and calving term (Fig. 3e), and therefore the Northern Hemisphere land ice gradually grows. The resulting slow increase in land albedo slowly reduces the temperature of the atmosphere and of the ocean (Fig. 3f) in the corresponding northern polar box. When the ocean sea-surface temperature (Fig. 3f) reaches the freezing temperature, sea ice forms very rapidly (Fig. 3b; 35 kyr). The creation of sea ice further increases the albedo, induces a further reduction of atmospheric temperature and results in the creation of more sea ice (positive feedback). In about 20 years, almost the entire northern polar box ocean surface is covered by sea ice. Dramatic sea-ice response to small climate changes has also been seen in previous studies (Thorndike, 1992; Flato and Brown, 1996). Sea ice stops growing when it isolates enough of the polar ocean from the cold atmosphere, reducing the air–sea cooling that leads to the sea-ice formation. The sea-ice “switch” is now turned to “on”. Note, though, that even during the model glacial maximum there is a strong seasonal cycle in the model sea-ice extension, so the sea-ice cover is significantly smaller during summer, consistent with recent proxy measurements (Weinelt and others, 1996).

At this stage, the average global temperature is at its lowest point, land ice-sheet and winter sea-ice extents are maximal, and the system is at a glacial maximum. The low atmospheric temperature reduces the poleward atmospheric moisture flux to about half its maximum value. Similarly, the sea-ice cover limits the moisture extraction from the polar ocean box and the corresponding snow accumulation over the land ice (Alley and others, 1993; Cuffey and Clow, 1997). As ablation, glacier melting, calving and runoff proceed as before (Fig. 3e), the glaciers start retreating. The albedo decreases again and the atmospheric temperature rises slowly. This is the beginning of the termination stage of the glacial period. Once the deep ocean warms enough and allows the upper ocean to warm as well, the sea ice melts within about 40 years (Fig. 3b; around 13 kyr). The sea-ice switch is now turned to “off”, the temperature of both the atmosphere and the ocean increases, and the system has completed a full glacial cycle.

Note that in this mechanism the glacial oscillations exist due to a self-sustained internal variability of the physical climate system. In Gildor and Tziperman (2000) we have shown that Milankovitch forcing provides only the phase locking of the 100 kyr variability. In Gildor and Tziperman (in press) we combine the physical climate system model with an ocean biochemistry model and variable atmos-

pheric CO₂. We show there that glacial–interglacial CO₂ variations amplify the glacial–interglacial cycles which exist even without the CO₂ variations. This amplifying role of the atmospheric CO₂ is consistent with the recent interpretation of the Vostok record (Petit and others, 1999).

The 100 kyr signal seen in proxy records is clearly global, but the precise phasing between them and the detailed mechanisms which connect the two hemispheres are still an open question (Clark and others, 1999). Changes in the intensity of the THC have been proposed as a way for the North Atlantic climate to affect to some degree the Southern Ocean. The present model shows a supplementary way in which Northern Hemisphere climate can be propagated to the Southern Hemisphere through the effects of NADW advected to the Southern Ocean. The temperature of the NADW is dictated by the amount of land ice in the northern box (Fig. 3a) through the albedo effect of the land ice on the Northern Hemisphere atmospheric and oceanic temperatures. As northern land ice expands, the temperature of the NADW forming in the northern box and flowing southward decreases (Fig. 3f–h), consistent with observations suggesting cooling of down to 4°C in the deep Tropical Atlantic (Schrag and others, 1996). Once reaching the Southern Ocean, the colder upwelling NADW (Fig. 3h) causes the sea-ice extension in the Southern Ocean to increase during glacial (Fig. 3c). This teleconnection mechanism between the two hemispheres through the temperature of the NADW supplements the possible mechanism that relies on the amplitude of the THC. Finally, we note that the changes to the temperature of the deep water in the Southern Ocean also affect the stratification and therefore the vertical mixing there. The effects of this mechanism on both the ocean biochemistry and the sea-ice extent are investigated in Gildor and Tziperman (in press).

4. CONCLUSION

This paper extends the sea-ice switch mechanism of the 100 kyr glacial–interglacial cycles (Gildor and Tziperman, 2000, 2001) to account for interhemispheric climate connectivity. In the interhemispheric teleconnection mechanism proposed here, cooling signals from the Northern Hemisphere, which result from the growth of Northern Hemisphere land-ice sheets, are transferred to the deep ocean by affecting the temperature of the NADW sinking in the northern high latitudes. The NADW cooling, in turn, is transported by the THC and affects the Southern Ocean. As sea-ice extension in the Southern Ocean is largely affected by the temperature of the deep-water upwelling there, the lower temperature of the deep water causes an increase in sea-ice extension (and albedo) in the Southern Hemisphere during glacial times.

An important aspect of the model solution is the occurrence of Northern Hemisphere sea ice in phase with the land-ice deglaciation. The model also predicts that deglaciation-related warming of the Southern Ocean may have occurred up to a few hundred years after that of the Northern Hemisphere, as this would be the time it takes the THC to transfer the signal from the Northern Hemisphere. There are some proxy data indications that the Southern Ocean warming of sea surface temperature may have occurred prior to the deglaciation of the Northern Hemisphere, at least on short time-scales (Labeyrie and others, 1996). Opposite proxy evidence for this interhemispheric phasing, more consistent with our results, exists as well (Steig and others, 1998; Clark

and others, 1999). In general, it seems that presently available sea-ice proxy data still lack the spatial and temporal resolution which would enable resolution of the sea-ice phase relative to that of the major land-ice deglaciation. Some studies suggest that at least a part of deglaciation has occurred during periods with extensive sea-ice cover (de Vernal and Pedersen, 1997; de Vernal and Hillaire-Marcel, 2000). Given the uncertainties of available proxy records, and especially given the lack of a satisfactory detailed physical mechanism for the glacial cycles (as opposed to just a fit to the available proxies) and for the teleconnection between the two hemispheres, we argue that it would be useful to keep an open mind regarding a possible sea-ice control of glacial dynamics, while examining both the available proxy record and new proxy data that become available.

The proposed mechanisms for both the 100 kyr glacial oscillations of Gildor and Tziperman (2000, 2001) and the interhemispheric teleconnection via deep-water temperature explored in this paper are clearly speculative at this stage, and it should be clear that we do not promote these as the only mechanism responsible for the 100 kyr glacial oscillations and for the synchronization of the two hemispheres. CO₂ feedbacks which could transfer information between the hemispheres (Genthon and others, 1987), or an explicit sea-level-glacier instability mechanism which could be especially important for the Antarctic ice sheet (Huybrechts and Oerlemans, 1990; Paterson, 1994) clearly contributed to globalizing climate changes. Another interhemispheric teleconnection mechanism not included here is the possible effect of Southern Ocean winds on the NADW formation rate (Toggweiler and Samuels, 1993). The omission of this mechanism may contribute to the small THC variability seen in our model (Fig. 3d). We wish to emphasize the need for a climate switch mechanism to supplement THC instabilities which do not seem to be able to account for global climate changes during glacial–interglacial cycles. Note that in the scenario proposed here, the THC plays an important role in the teleconnection between the hemispheres, but it is the sea-ice switch that shifts the climate system from one phase of the glacial oscillation to another. Fuller general circulation models and new sea-ice proxy data are clearly needed to quantify the relative role of the proposed role of sea ice and of the deep THC temperature.

ACKNOWLEDGEMENTS

We thank M. A. Morales Maqueda, M. Montoya and an anonymous reviewer for their most useful and constructive comments. This work is partially supported by the Israeli–U.S. Binational Science Foundation.

REFERENCES

Alley, R. B. and 10 others. 1993. Abrupt increase in Greenland snow accumulation at the end of the Younger Dryas event. *Nature*, **362**(6420), 527–529.

Broecker, W. S. and G. H. Denton. 1989. The role of ocean–atmosphere reorganizations in glacial cycles. *Geochim. Cosmochim. Acta*, **53**(10), 2465–2501.

Charles, C. D., R. Rind, J. Jouzel, R. D. Koester and R. G. Fairbanks. 1994. Glacial–interglacial changes in moisture sources for Greenland: influences on the ice core record of climate. *Science*, **263**(5146), 508–511.

Clark, P. U., R. B. Alley and D. Pollard. 1999. Northern Hemisphere ice-sheet influences on global climate change. *Science*, **286**(5442), 1104–1111.

Crowley, T. J. and G. R. North. 1991. *Paleoclimatology*. Oxford, etc., Oxford University Press. (Oxford Monographs on Geology and Geophysics 18.)

Cuffey, K. M. and G. Clow. 1997. Temperature, accumulation, and ice sheet elevation in central Greenland through the last deglacial transition. *J.*

Geophys. Res., **102**(C12), 26,383–26,396.

De Vernal, A. and C. Hillaire-Marcel. 2000. Sea-ice cover, sea-surface salinity and halo-/thermocline structure of the northwest North Atlantic: modern versus full glacial condition. *Quat. Sci. Rev.*, **19**(1–5), 65–85.

De Vernal, A. and T. Pedersen. 1997. Micropaleontology and palynology of core PAR87A-10: a 23,000 year record of paleoenvironmental changes in the Gulf of Alaska, northeast North Pacific. *Paleoceanography*, **12**(6), 821–830.

Donn, W. L. and M. Ewing. 1966. A theory of ice ages III. *Science*, **152**(3730), 1706–1712.

Flato, G. M. and R. D. Brown. 1996. Variability and climate sensitivity of landfast Arctic sea ice. *J. Geophys. Res.*, **101**(C11), 25,767–25,778.

Genthon, C. and 7 others. 1987. Vostok ice core: climatic response to CO₂ and orbital forcing changes over the last climatic cycle. *Nature*, **329**(6138), 414–418.

Ghil, M. 1994. Cryothermodynamics: the chaotic dynamics of paleoclimate. *Physica D*, **77**(1–3), 130–159.

Ghil, M., A. Mullhaupt and P. Pestiaux. 1987. Deep water formation and Quaternary glaciations. *Climate Dyn.*, **2**(1), 1–10.

Gildor, H. and E. Tziperman. 2000. Sea ice as the glacial cycles climate switch: role of seasonal and Milankovitch solar forcing. *Paleoceanography*, **15**(6), 605–615.

Gildor, H. and E. Tziperman. 2001. A sea-ice climate-switch mechanism for the 100 kyr glacial cycles. *J. Geophys. Res.*, **106**(C5), 9117–9133.

Gildor, H. and E. Tziperman. In press. Physical mechanisms behind biogeochemical glacial–interglacial CO₂ variations. *Geophys. Res. Lett.*

Gnanadesikan, A. 1999. A simple predictive model for the structure of the oceanic pycnocline. *Science*, **283**(5410), 2077–2079.

Gordon, A. L. 1981. Seasonality of Southern Ocean ice. *J. Geophys. Res.*, **86**(C5), 4193–4197.

Haney, R. L. 1971. Surface thermal boundary condition for ocean circulation models. *J. Phys. Oceanogr.*, **1**(4), 241–248.

Hebbeln, D., T. Dokken, E. Andersen, M. Hald and A. Elverhoi. 1994. Moisture supply for northern ice-sheet growth during the Last Glacial Maximum. *Nature*, **370**(6488), 357–360.

Huybrechts, P. and J. Oerlemans. 1990. Response of the Antarctic ice sheet to future greenhouse warming. *Climate Dyn.*, **5**(2), 93–102.

Huybrechts, P., A. Letréguilly and N. Reeh. 1991. The Greenland ice sheet and greenhouse warming. *Global and Planetary Change*, **3**(4), 399–412.

Imbrie, J. and 18 others. 1993. On the structure and origin of major glaciation cycles. 2. The 100,000-year cycle. *Paleoceanography*, **8**(6), 699–735.

Källén, E., C. Crafoord and M. Ghil. 1979. Free oscillations in a climate model with ice-sheet dynamics. *J. Atmos. Sci.*, **36**(12), 2292–2303.

Labeyrie, L. and 11 others. 1996. Hydrographic changes of the Southern Ocean (southeast Indian sector) over the last 230 kyr. *Paleoceanography*, **11**(1), 57–76.

Le Treut, H. and M. Ghil. 1983. Orbital forcing, climatic interactions, and glaciations cycles. *J. Geophys. Res.*, **88**(C9), 5167–5190.

Lorius, C. and 6 others. 1985. A 150,000-year climatic record from Antarctic ice. *Nature*, **316**(6029), 591–596.

Loutre, M.-F. and A. Berger. 2000. No glacial–interglacial cycle in the ice volume simulated under a constant astronomical forcing and a variable CO₂. *Geophys. Res. Lett.*, **27**(6), 783–786.

Manabe, S. and A. J. Broccoli. 1985. The influence of continental ice sheets on the climate of an ice age. *J. Geophys. Res.*, **90**(D1), 2167–2190.

Martinson, D. G. 1990. Evolution of the Southern Ocean winter mixed layer and sea ice: open ocean deepwater formation and ventilation. *J. Geophys. Res.*, **95**(C7), 11,641–11,654.

Maykut, G. A. and D. K. Perovich. 1987. The role of shortwave radiation in the summer decay of a sea ice cover. *J. Geophys. Res.*, **92**(C7), 7032–7044.

Muller, R. A. and G. J. MacDonald. 1997. Glacial cycles and astronomical forcing. *Science*, **277**(5323), 215–218.

Paillard, D. 1998. The timing of Pleistocene glaciations from a simple multiple-state climate model. *Nature*, **391**(6665), 378–381.

Paterson, W. S. B. 1994. *The physics of glaciers. Third edition*. Oxford, etc., Elsevier.

Peltier, W. R. 1994. Ice age paleotopography. *Science*, **265**(5169), 195–201.

Peltier, W. R. and S. Marshall. 1995. Coupled energy-balance/ice-sheet model simulations of the glacial cycle: a possible connection between terminations and terrigenous dust. *J. Geophys. Res.*, **100**(D7), 14,269–14,289.

Petit, J.-R. and 18 others. 1999. Climate and atmospheric history of the past 420,000 years from the Vostok ice core, Antarctica. *Nature*, **399**(6735), 429–436.

Pollard, D. 1983. A coupled climate–ice sheet model applied to the Quaternary ice ages. *J. Geophys. Res.*, **88**(C12), 7705–7718.

Ruddiman, W. F. and A. McIntyre. 1981. Oceanic mechanisms for amplification of the 23,000-year ice-volume cycle. *Science*, **212**(4495), 617–627.

Saltzman, B. 1990. Three basic problems of paleoclimate modeling: a personal perspective and review. *Climate Dyn.*, **5**(5), 67–88.

Saltzman, B. and M. Y. Verbitsky. 1993. Multiple instabilities and modes of glacial rhythmicity in the Plio-Pleistocene: a general theory of Late

- Cenozoic climatic change. *Climate Dyn.*, **9**(1), 1–15.
- Schrag, D. P., G. Hampt and D. Murray. 1996. Pore fluid constraints on the temperature and oxygen isotopic composition of the glacial ocean. *Science*, **272**(5270), 1930–1932.
- Steig, E. J. and 8 others. 1998. Synchronous climate changes in Antarctica and the North Atlantic. *Science*, **282**(5386), 92–95.
- Stokes, W. L. 1955. Another look at the ice age. *Science*, **122**(3174), 815–821.
- Stommel, H. 1961. Thermohaline convection with two stable regimes of flow. *Tellus*, **13**(2), 224–230.
- Thorndike, A. S. 1992. A toy model linking atmospheric thermal radiation and sea ice growth. *J. Geophys. Res.*, **97**(C6), 9401–9419.
- Toggweiler, J. R. and B. Samuels. 1993. Is the magnitude of the deep outflow from the Atlantic Ocean actually governed by Southern Hemisphere winds? In Heimann, M., ed. *The global carbon cycle*. Berlin, etc., Springer-Verlag, 303–331. (NATO ASI Series I: Global Environmental Change 15.)
- Unesco. 1981. *10th report of the joint panel on oceanographic tables and standards*. Paris, Unesco. Joint Panel on Oceanographic Tables and Standards. (Technical Report 36.)
- Weaver, A. J., M. Eby, A. Fanning and E. C. Wiebe. 1998. Simulated influence of carbon dioxide, orbital forcing and ice sheets on the climate of the Last Glacial Maximum. *Nature*, **394**(6696), 847–853.
- Weertman, J. 1976. Milankovitch solar radiation variations and ice age ice sheet sizes. *Nature*, **261**(5555), 17–20.
- Weinelt, M., M. Sarnthein, U. Pflaumann, H. Schultz, S. Jung and H. Erlenkeuser. 1996. Ice-free Nordic seas during the Last Glacial Maximum? Potential sites of deepwater formation. *Palaeoclimates*, **1**, 282–309.